ISSN 1063-7710, Acoustical Physics, 2014, Vol. 60, No. 2, pp. 148–154. © Pleiades Publishing, Ltd., 2014.

CLASSICAL PROBLEMS OF LINEAR ACOUSTICS AND WAVE THEORY

Transmission Mode of One-Dimensional Phononic Crystal Based on Coupling of Total Evanescent Waves[1]

Yun-tuan Fang[a], Ji-jun Wang[b], and Ying-xin Jiang[b]

[a]*School of Computer Science and Telecommunication Engineering, Jiangsu University, Zhenjiang, 212013 P.R. China*

[b]*Department of Physics, Jiangsu University, Zhenjiang, 212013 P.R. China*

e-mail: fang_yt1965@sina.com

Received March 4, 2013

Abstract—In order to obtain the transmission properties of one-dimensional phononic crystal under total evanescent waves, we design structure model. Basing on the basic acoustic wave equations and boundary condition as well as the Bloch theory, we study the band structure of one-dimensional phononic crystal. We summarize the properties of the mode based on the coupling of total evanescent waves and explain its physical mechanism. There are three transmission modes in phononic crystal. Based on the coupling of total evanescent waves, the number of perfect transmission peaks is just equal to the number of structure period, and the thickness of period can be much less than the wave length.

Keywords: phononic crystal, evanescent waves, transmission mode

DOI: 10.1134/S1063771014020043

1. INTRODUCTION

Classical waves in periodic material structure have the band gap structures just as those of electronics in semiconductor lattice [1–4]. Corresponding to different classical waves, people have proposed the concepts of photonic crystals and phononic crystals. The main properties of photonic crystals and phononic crystals are their band gap structures. The waves can be transmitted in the bands and are prohibited in the gaps. Any waves follow the Bloch theory in an ideal periodic structure [5], i.e., they exist in the form of Bloch waves. The study of phononic crystals is usually with the help of the study methods for photonic crystals. However, acoustic waves and electromagnetic waves are different in physics. Especially, acoustic waves have two forms of transverse wave and longitudinal wave in solid materials. Thus phononic crystals and photonic crystals have different transmission properties. Although people have carried out extensive and deep study on photonic crystals and phononic crystals [6–9], it does not mean that such study has come to its end. With the emergence of new materials and new structure models, the research domain may often open a new door, for example, the study of negative refraction of photonic crystals and phononic crystals in recent years [10, 11]. For the forming mechanism of band gaps of photonic crystals and phononic crystals, the traditional theory attributes them to Bragg scatter [4] and local resonances [8]. Liu and we proposed a new transmission mechanism of photonic crystals and phononic crystals based on the effect of photon or phonon tunneling [12–15]. It shows that classical waves can be transmitted in layered structure on the condition of total reflection. Following the ideas of [12–15], we further propose a transmission mode which based on the coupling of total evanescent waves in this study. Compared with the traditional transmission modes, our transmission mode takes on some unique features which have not been found in published papers.

2. MODEL AND METHOD

Figure 1 is the schematic of one-dimensional phononic crystal (1D PC). The whole structure is

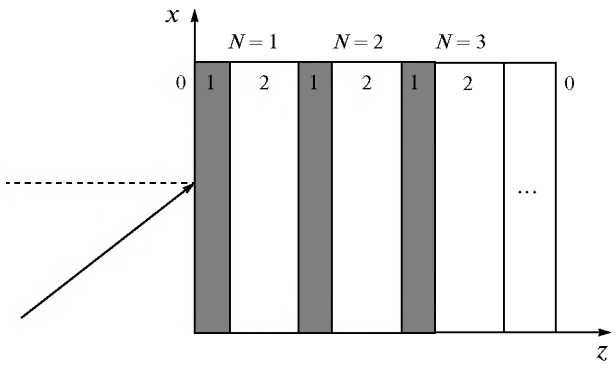

Fig. 1. Schematic of one-dimensional phononic crystal in the background of air (0). 1 and 2 are glass and water, respectively. N is the period number.

[1] The article is published in the original.

placed along the z axis and in the background of air 0. 1 and 2 are the solid and liquid media, respectively. N is the period number. The densities, velocities and thicknesses for layers 1 and 2 are denoted as ρ_1, ρ_2, v_{1L}, v_{1T}, v_{2L}, d_1, d_2, respectively, where the subscripts L and T denote transverse waves and longitudinal waves. The period length is $d = d_1 + d_2$. The density and velocity for the background media are ρ_0 and v_{0L}. For layer 2 and the background media, there are only longitudinal waves. The plane acoustic waves propagate in the xoz plane. After multiple refractions and reflections, the displacement field within each layer is a superposition of transmitted and reflected waves as shown in Fig. 2. Within layer 1, the displacements for transverse waves and longitudinal waves are denoted as

$$A_1 = A_1^+ \exp[i(k_{1L}\cos\theta_{1L}z + k_{1L}\sin\theta_{1L}x - \omega t)] \quad (1)$$

$$B_1 = B_1^- \exp[i(-k_{1L}\cos\theta_{1L}z + k_{1L}\sin\theta_{1L}x - \omega t)] \quad (2)$$

$$C_1 = C_1^+ \exp[i(k_{1T}\cos\theta_{1T}z + k_{1T}\sin\theta_{1T}x - \omega t)] \quad (3)$$

$$D_1 = D_1^- \exp[i(-k_{1T}\cos\theta_{1T}z + k_{1T}\sin\theta_{1T}x - \omega t)] \quad (4)$$

where "+" and "−" denote transmitted and reflected waves, respectively. Within layer 2, the displacements for longitudinal waves are denoted as

$$A_2 = A_2^+ \exp[i(k_{2L}\cos\theta_{1L}z + k_{2L}\sin\theta_{1L}x - \omega t)], \quad (5)$$

$$B_2 = B_2^- \exp[i(-k_{2L}\cos\theta_{2L}z + k_{2L}\sin\theta_{2L}x - \omega t)]. \quad (6)$$

In all equations, ω is angular frequency, $k_L = \omega/v_L$ and $k_T = \omega/v_T$ are the wave vectors, v_L and v_T are the velocities, θ_L and θ_T are the angles between propagating direction and z axis. The stress is given by use of Hooker's law

$$\sigma_{zz} = \lambda\left(\frac{\partial U_z}{\partial z} + \frac{\partial U_x}{\partial x}\right) + 2\mu\frac{\partial U_z}{\partial z}, \qquad \sigma_{zx} = \mu\left(\frac{\partial U_x}{\partial z} + \frac{\partial U_z}{\partial x}\right), \quad (7)$$

where U_x and U_z are the displacement components in the x and z directions. λ and μ are Lame's constants which satisfy the following equation:

$$\lambda + 2\mu = \rho c_L^2, \quad \mu = \rho c_T^2. \quad (8)$$

In liquid $\mu = 0$. Continuity of displacement at the interface gives:

$$\cos\theta_{1L}A_1 - \cos\theta_{1L}B_1 + \sin\theta_{1T}C_1 + \sin\theta_{1T}D_1 = \cos\theta_{2L}A_2 - \cos\theta_{2L}B_2. \quad (9)$$

Continuity of stress at the interface gives

$$ik_{1L}(\lambda_1 + 2\mu_1\cos^2\theta_{1L})A_1 + ik_{1L}(\lambda_1 + 2\mu_1\cos^2\theta_{1L})B_1 + (ik_{1T}\mu_1\sin 2\theta_{1T}C_1 - ik_{1T}\mu_1\sin 2\theta_{1T}D_1) = ik_{2L}\lambda_2 A_2 + ik_{2L}\lambda_2 B_2. \quad (10)$$

If we neglect the viscosity of liquid, the displacement and stress components in the x direction in layer 2 cannot be transmitted into layer 1. Thus the displacement and stress components in the x direction in layer 1 are both zero. From $U_{jx} = 0$ and $\mu\left(\frac{\partial U_{1x}}{\partial z} + \frac{\partial U_{1z}}{\partial x}\right) = 0$, we have

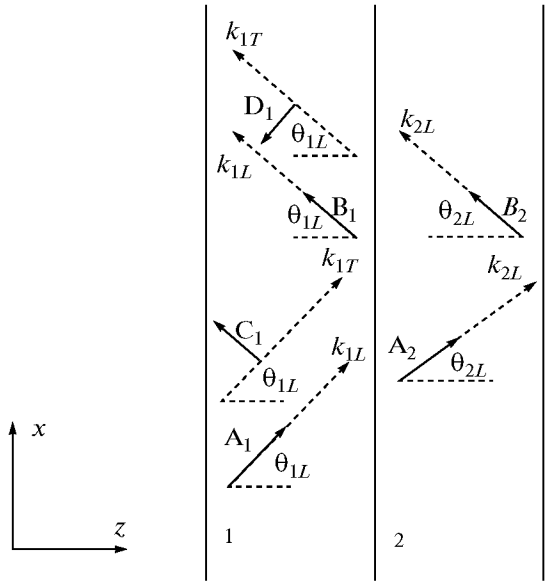

Fig. 2. The transversal wave and longitudinal wave in the multilayers.

$$C_1 - D_1 = [\sin\theta_{1L}/\cos\theta_{1T}](A_1 + B_1), \quad (11)$$

$$C_1 + D_1 = [k_{1L}\sin 2\theta_{1L}/(k_{1T}\cos 2\theta_{1T})](A_1 - B_1). \quad (12)$$

From Eqs. (11) and (12), we obtain

$$C_1 = \left[\frac{\sin\theta_{1L}}{\cos\theta_{1T}} + \frac{k_{1L}\sin 2\theta_{1L}}{k_{1T}\cos 2\theta_{1T}}\right]A_1/2 + \left[\frac{\sin\theta_{1L}}{\cos\theta_{1T}} - \frac{k_{1L}\sin 2\theta_{1L}}{k_{1T}\cos 2\theta_{1T}}\right]B_1/2, \quad (13)$$

$$D_1 = -\left[\frac{\sin\theta_{1L}}{\cos\theta_{1T}} - \frac{k_{1L}\sin 2\theta_{1L}}{k_{1T}\cos 2\theta_{1T}}\right]A_1/2 - \left[\frac{\sin\theta_{1L}}{\cos\theta_{1T}} + \frac{k_{1L}\sin 2\theta_{1L}}{k_{1T}\cos 2\theta_{1T}}\right]B_1/2. \quad (14)$$

After Eqs. (13) and (14) are taken into Eqs. (9) and (10), the acoustic waves in one-dimensional solid–liquid phononic crystal are united into longitudinal waves. According to the idea of transfer matrix for layered structures [3], we use

$$U_{Ni} = \begin{bmatrix} A_{Ni} \\ B_{Ni} \end{bmatrix} \quad (i = 1, 2) \quad (15)$$

denoting the displacement from the two sides of interface (N is the period number). Eqs. (9) and (10) can be written as [13]

$$M_1 U_{N1} = M_2 U_{N2}, \quad (16)$$

where

$$M_1=\begin{bmatrix} \cos\theta_{1L}+\dfrac{k_{1L}\sin\theta_{1T}\sin2\theta_{1L}}{k_{1T}\cos2\theta_{1T}} & -\left(\cos\theta_{1L}+\dfrac{k_{1L}\sin\theta_{1T}\sin2\theta_{1L}}{k_{1T}\cos2\theta_{1T}}\right) \\ ik_{1L}(\lambda_1+2\mu_1\cos^2\theta_{1L})+2ik_{1T}\mu_1\sin\theta_{1T}\sin\theta_{1L} & ik_{1L}(\lambda_1+2\mu_1\cos^2\theta_{1L})+2ik_{1T}\mu_1\sin\theta_{1T}\sin\theta_{1L} \end{bmatrix},$$

$M_2 = \begin{bmatrix} \cos\theta_{2L} & -\cos\theta_{2L} \\ ik_{2L}\lambda_2 & ik_{2L}\lambda_2 \end{bmatrix}$ are called dynamical matrix for layers 1 and 2. Thus we obtain the relation of displacements at the two interfaces of one period:

$$\begin{aligned} M_1U_{N1} &= M_2P_2M_2^{-1}M_1P_1U_{(1+N)1} \\ &= (M_2G_2M_2^{-1}M_1G_1M_1^{-1})M_1U_{(1+N)1} \\ &= MM_1U_{(1+N)1}, \end{aligned} \tag{17}$$

where

$$G_1 = \begin{bmatrix} \exp(-ik_{1L}d_1\cos\theta_{1L}) & 0 \\ 0 & \exp(ik_{1L}d_1\cos\theta_{1L}) \end{bmatrix},$$

$$G_2 = \begin{bmatrix} \exp(-ik_{2L}d_2\cos\theta_{2L}) & 0 \\ 0 & \exp(ik_{2L}d_2\cos\theta_{2L}) \end{bmatrix},$$

and $M = M_2G_2M_2^{-1}M_1G_1M_1^{-1}$. According to the Bloch theory of periodic structure

$$U_{(1+N)1} = \exp(iKd)U_{N1}, \tag{18}$$

where K is Bloch wave vector. Thus Eq. (17) becomes

$$MX = \exp(-iKd)X, \tag{19}$$

where $X = M_1U_{(N)1}$. Eq. (19) is an eigen equation of matrix. Because of $|M| = 1$, the eigen values of Eq. (19) are $\exp(Kd)$ and $\exp(-iKd)$, respectively. Thus we have

$$\cos(Kd) = [M(1,1)+M(2,2)]/2. \tag{20}$$

The condition that Eq. (20) has real solution is $|\cos(Kd)| \le 1$. Acoustic waves satisfying $|\cos(Kd)| \le 1$ become transmitted wave forming transmission band, otherwise K is imaginary number forming forbidden band and acoustic waves in the phononic crystal are the evanescent Bloch waves. In Fig. 1, acoustic wave is incident on the PC with angular frequency ω and incidence angle θ_{0L}. The wave vector in the air $k_{0L} = \dfrac{\omega}{v_{0L}}$ has a component in the x direction $k_x = \dfrac{\omega}{v_{0L}}\sin\theta_{0L}$ which keeps invariant in each layer. According to k_x, we obtain the incidence angles in each layer:

$$\theta_{0L} = \arccos\sqrt{1-\frac{k_x^2}{k_{0L}^2}}, \quad \theta_{1L} = \arccos\sqrt{1-\frac{k_x^2}{k_{1L}^2}},$$

$$\theta_{1T} = \arccos\sqrt{1-\frac{k_x^2}{k_{1T}^2}}, \quad \theta_{2L} = \arccos\sqrt{1-\frac{k_x^2}{k_{2L}^2}}.$$

For given structure parameters, Eq. (20) is only dependent on ω and k_x, which determines the structure of band gap. For finite period structure, we can deduce the transmission coefficient. $U_0 = \begin{bmatrix} A_0 \\ B_0 \end{bmatrix}$ is the displacement on the incident interface between the air and layer 1 and $U_{N0} = \begin{bmatrix} A_{N0} \\ B_{N0} \end{bmatrix}$ is the displacement on the transmitted interface between the air and layer 2. The relation between them is

$$\begin{aligned} \begin{bmatrix} A_0 \\ B_0 \end{bmatrix} &= M_0^{-1}(M_1G_1M_1^{-1}M_2G_2M_2^{-1})^N \\ &\times M_0\begin{bmatrix} A_{N0} \\ B_{N0} \end{bmatrix} = M_N\begin{bmatrix} A_{N0} \\ B_{N0} \end{bmatrix}, \end{aligned} \tag{21}$$

where $M_0 = \begin{bmatrix} \cos\theta_{0L} & -\cos\theta_{0L} \\ ik_{0L}\lambda_0 & ik_{0L}\lambda_0 \end{bmatrix}$, $M_N = P_0^{-1}(M_1G_1M_1^{-1}M_2G_2M_2^{-1})^N$. Because of $B_{N0} = 0$, the transmission coefficient is

$$T = \left|\frac{A_{N0}}{A_0}\right| = \left|\frac{1}{M_N(1,1)}\right|. \tag{22}$$

3. CALCULATIONS AND MODE ANALYSIS

For the structure model, we choose $\rho_0 = 1.29$ kg/m^3, $\rho_1 = 1180$ kg/m^3, $\rho_2 = 1000$ kg/m^3, $v_{0L} = 330$ m/s, $v_{1L} = 2670$ m/s, $v_{1T} = 1120$ m/s, $v_{2L} = 1500$ m/s, $d_1 = 1$ mm, $d_2 = 4$ mm. Because the acoustic velocity in the air is very small, there are three modes:

(1) $k_x < k_{1L}$, $k_x < k_{2L}$ (Mode I);

(2) $k_x > k_{1L}$, $k_x < k_{2L}$ (Mode II);

(3) $k_x > k_{1L}$, $k_x > k_{2L}$ (Mode III).

Mode I is a traditional transmission mode. The z components of k_{1L} and k_{2L} are both real number. There are all propagating waves in all layers. The transmission mechanism is the Bragg scatter of periodic structure or local resonances. Mode II is the same as those proposed in refs. [12–15]. The z components of k_{1L} and k_{2L} are complex number and real number, respectively. Thus the acoustic waves in layer 1and layer 2 are evanescent and propagating, respectively. In general, evanescent waves cannot propagate perpendicularly to the interface. In current structure, the wavelength in each layer is larger than the layer's thickness. Thus in the first structure period the field

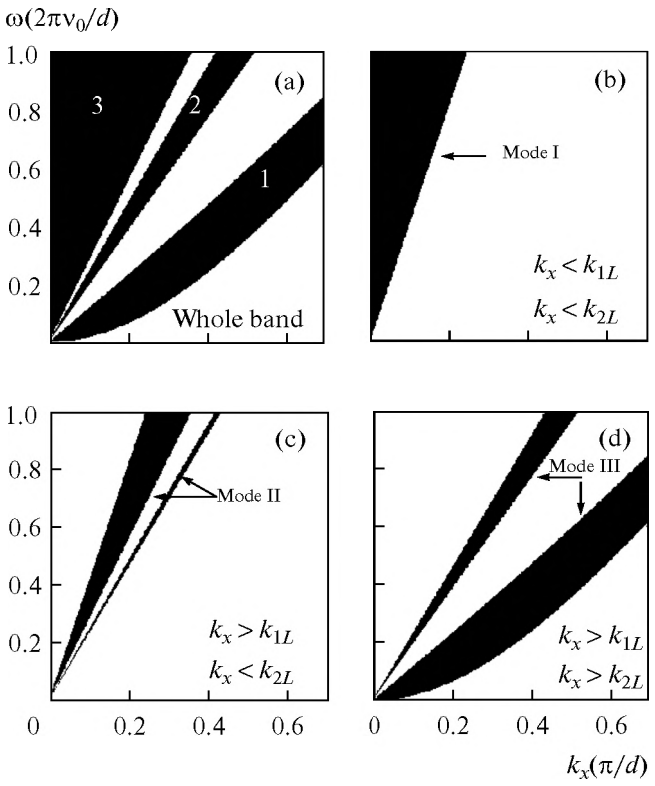

Fig. 3. Band structure of the one-dimensional phononic crystal under different conditions.

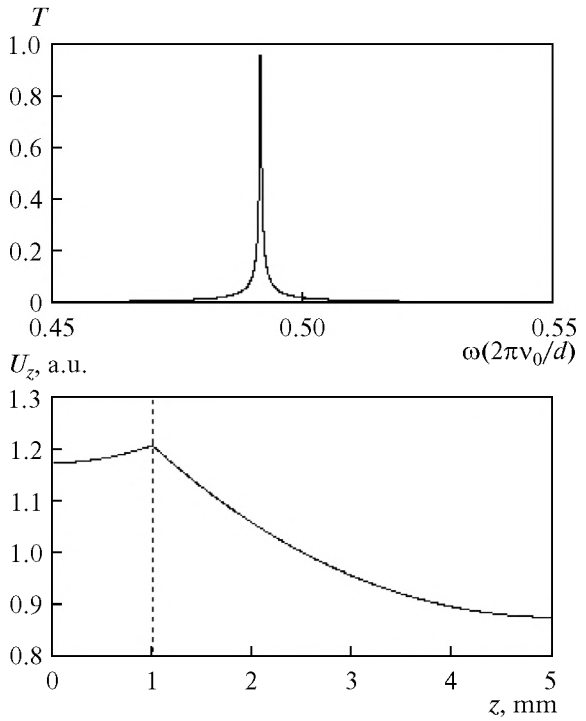

Fig. 4. Transmission spectrum of the one-dimensional phononic crystal with single period for mode III in the first band (top plot) and distributions of displacement field corresponding to the peak frequency at top plot (bottom plot). The dotted line denotes the inner interface.

can reaches the last interface of the period and undergoes reflection. The reflected field and the transmitted field take resonance at the interface between layers 1 and 2 forming a resonant cavity. The energy of resonance makes the evanescent waves penetrate into the next structure period and so on. Thus a resonance tunneling effect occurs. Mode III has not been reported and is the main subject of this paper. Because the z components of k_{1L} and k_{2L} are both complex number meaning that the waves in all layers are evanescent. On this case, whether the acoustic waves can be transmitted is dependent on the right side value of Eq. (20). Thus we make some calculations and the results are shown in Fig. 3. For comparison, we also take small values of k_x. In all figures, the black part and the white part denote the transmission band and the prohibited band, respectively. Figure 3a is the whole band structure. For a definite k_x, the lower transmission band is called Band 1 and the others are called Band 2 and Band 3. In Fig. 3b ($k_x < k_{1L}$, $k_x < k_{2L}$), the transmission band corresponds to Mode I which is totally within Band 3. In Fig. 3c ($k_x > k_{1L}$, $k_x < k_{2L}$), the transmission band corresponds to Mode II which are localized in Band 2 and Band 3, respectively. In Fig. 3d ($k_x > k_{1L}$, $k_x > k_{2L}$), the transmission band corresponds to Mode III which are localized in Band 1 and Band 2, respectively. Figure 3d shows that transmission bands still occur even if the waves in all layers are evanescent. This is a new transmission mode. Before we study the transmission mechanism of Mode III, we study the transmission spectra and the distributions of displacement field of Mode III for finite 1D PC. Although Fig. 3 is based on infinite structure, the transmission spectra for finite period number are still in agreement with those of Fig. 3.

Without loss of generality, we choose $k_x = 0.4\ \pi/d$. Firstly, we consider the structure with a single period. Figure 4 (top plot) shows the transmission spectrum of Mode III in Band 1. A perfect transmission peak occurs within a wide gap background. Here we give the reasons that the forming of the peak. The evanescent field can penetrate from the front interface to the back interface of the structure because the wavelength in the structure is much larger than the thickness of each layer. The differences of the impedances (ρν) among matrix material and the material in phononic crystal are very big, which results in intense reflection on both the front interface to the back interface. The forward evanescent field and backward evanescent field meet at the inner interface. A resonance occurs at the middle interface because there is no phase change for evanescent fields. Figure 4 (bottom plot) shows the distributions of displacement field corresponding to the peak frequency at top plot (bottom plot). It is clear that the displacement field has the maximum value at the inner interface, which verifies our above analysis.

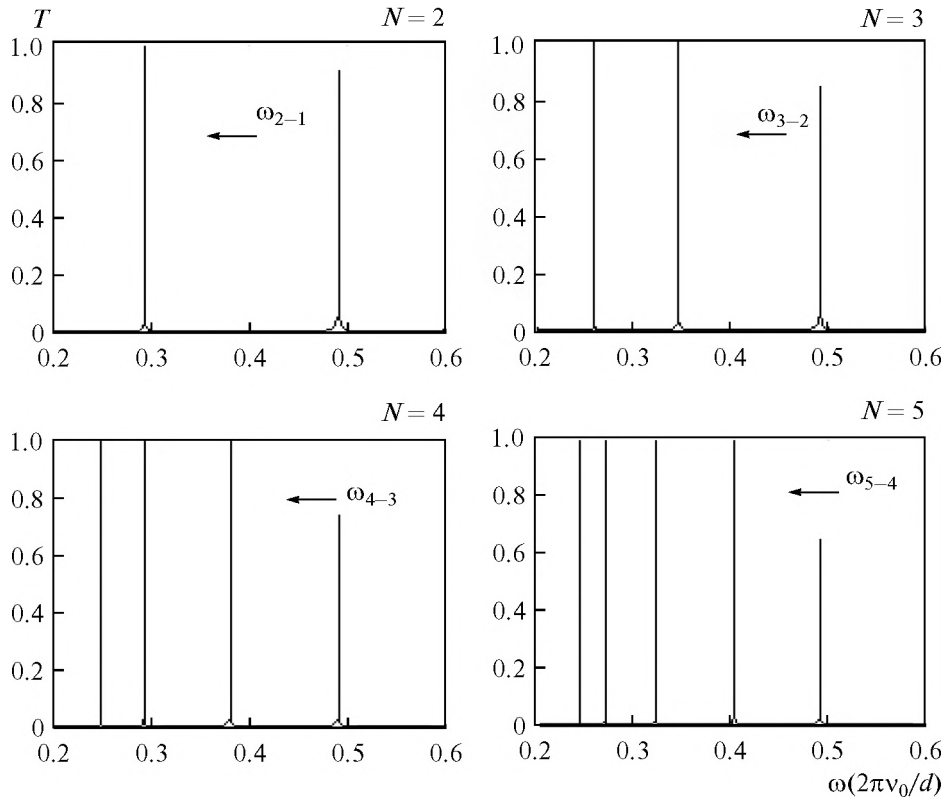

Fig. 5. Transmission spectrum of the one-dimensional phononic crystal with different periods for $k_x = 0.4\pi/d$ in the first band. ($\omega_{2-1} = 0.29298(2\pi\nu_0/d)$, $\omega_{3-2} = 0.34618(2\pi\nu_0/d)$, $\omega_{4-3} = 0.3838(2\pi\nu_0/d)$, $\omega_{5-4} = 0.40346(2\pi\nu_0/d)$.

Figure 5 further shows the dependence of the transmission coefficient on the angular frequency for Mode III in Band 1. The transmission spectra have following features.

First, the transmission band consists of N discrete narrow perfect peaks. It is similar to the transmission band for Mode II in [12–15], in which there are $N-1$ discrete narrow peaks. It is totally different from the transmission band of Mode I in traditional 1D PC in which the transmission band consists of some mini-bands and mini-gaps.

Second, the intervals among the peaks are different. The larger the frequency, the larger the intervals.

Third, the positions of the peaks at the right outside in each sub-plot are all the same. The peaks at the right outside are close to the up edge of Band 1 insensitive to the number of period and have peak values smaller than 1. For Mode II with odd peak number, the position of the middle peak keeps invariant [12, 13, 15].

Fourth, except the outside peak, all transmission peaks have unit peak value. All the positions of these peaks are dependent on N. The peak position for the peak ω_{N-i} (N is the period number, i denotes the ith peak from the left) keeps invariant when N increases with integral times. For example, the peak position for ω_{2-1} keeps invariant when $N = 4, 6, 8, \ldots$, or the peak position for ω_{4-1} keeps invariant when $N = 4, 8, 12, \ldots$.

Figure 6 shows the transmission spectra within Band 2 for $k_x = 0.4\ \pi/d$ and different N. Because Band 2 includes Mode II and Mode III, the transmission peaks in it are within to different transmssion modes. The left group is within Mode III and the right group is within Mode II. The total number of peaks is $N-1$.

Figure 7 shows the distributions of displacement field corresponding to different peak frequencies (pointed by arrows) in Fig. 5 with $N = 20$ and $d = 5$ mm. The amplitude of incident wave is assumed as 1 with no dimension. All the field distributions take on the clear characteristics of Bloch waves, that is, they change periodically. For peaks ω_{2-1}, ω_{3-2}, ω_{4-3} and ω_{5-4}, the periods of fields are $2d$, $3d$, $4d$ and $5d$, respectively. Such result is similar to that of Mode II which can be explained through effective Bloch wave vector [12]. The feature of field distribution also illustrates that the position of peak $N-i$ keeps invariant when N increases with integral times. We also notice that the maximum value of field is always located at the interface which is just the result of local resonance at the interface.

The transmission spectra and field distributions illustrate that the transmission mechanism of current

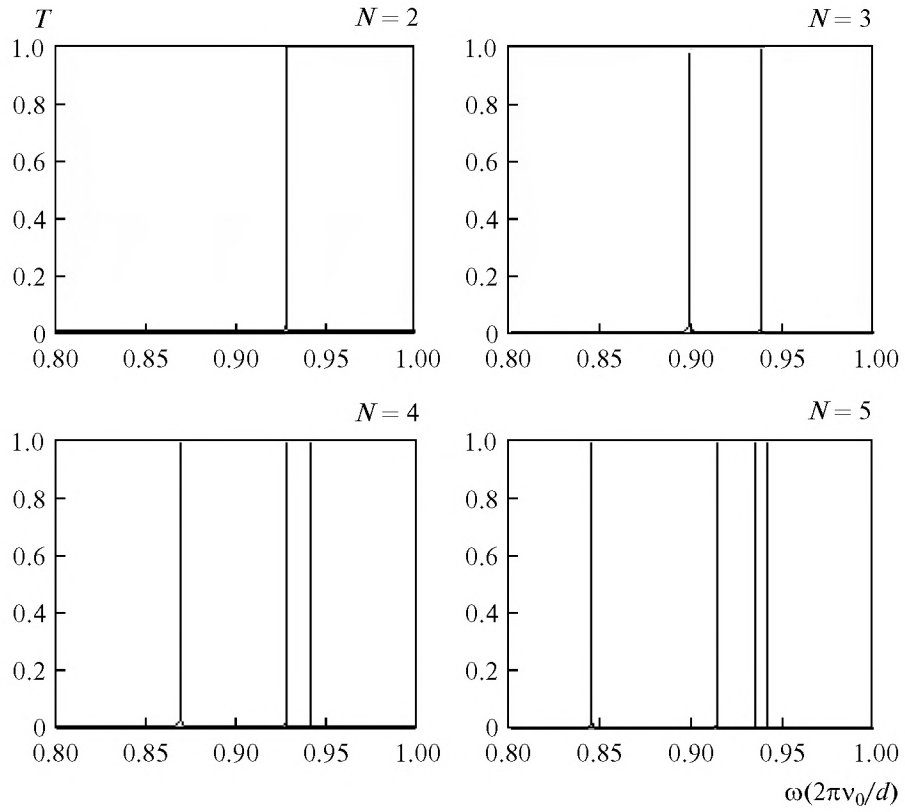

Fig. 6. Transmission spectrum of the one-dimensional phononic crystal with different periods for $k_x = 0.4\pi/d$ in Band 2.

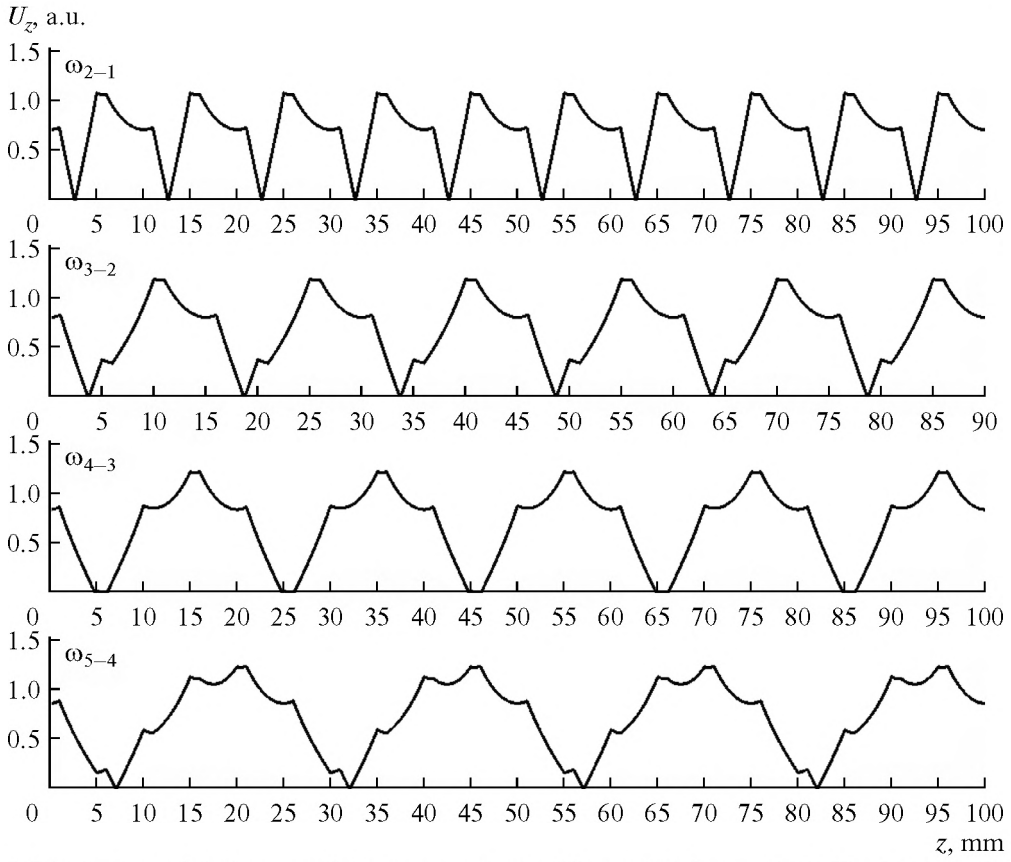

Fig. 7. Distributions of displacement field corresponding to different peak frequencies in Fig. 5 with $d = 5$ mm.

1D PC is attributed to both the effects of Bragg scatter and local resonance. As mentioned above, a single period can form the mode of local resonance. For structure with multiple periods, these local resonance modes are coupled through evanescent field. The coupling makes the single local resonance mode split and forms the band. The position of the band is determined by Fig. 3. According to the classical wave analog of the tight-binding (TB) model, a single local resonance mode is split into N modes. If the coupling is weaker, the N modes form a successive band, otherwise form a discrete band. The result in this study corresponds to the latter. The resonant unit for Mode III is different from that for Mode II introduced in Refs. [12–16]. The resonance unit for Mode II is achieved through standing wave resonance within one layer of the structure period. The maximum value of field is always located within the layer. The resonance unit for Mode III is achieved through the resonance of evanescent waves in the whole period. The maximum value of field is located at the interface. Because the resonance unit for Mode II must satisfy the resonant condition of standing waves, the wavelength should be the same order as the thickness of media layer. However, the wavelength for Mode III can be much larger than the length of the resonance unit. For example, the wavelengths in layers 1 and 2 for peak $\omega_{2-1} = 0.29298(2\pi v_0/d)$ are 138.07 mm and 77.57 mm, respectively, which are much larger than the period length 5 mm. The classical waves can be still transmitted in Mode III through one-dimensional photonic crystal [17]. In ref. [17], the electromagnetic waves are transmitted along the normal direction through the coupling of evanescent waves in one-dimensional photonic crystal.

All the results show that 1D PC takes on some special properties when acoustic waves propagate in it in Mode III. Its comb discrete channels are not limited to the number of periods. Only single period can achieve one filtering channel with high Q values, while for traditional 1D PC, only with enough period number can it achieve filtering channels. For Mode III the period length can be much smaller than wavelength, which means that the structure with small size can control the large wavelength.

4. CONCLUSIONS

We have deduced the band structure of 1D PC through the basic equations of acoustic waves and boundary conditions. We find a new kind of transmission mechanism for 1D PC called the coupling of total evanescent waves. Through calculating the transmission spectra and the field distributions, we analyze the physical mechanism and conclude its special properties for such mechanism. Our study may extend the theoretical and application domain of 1D PC.

REFERENCES

1. E. Yablonovitch, Phys. Rev. Lett. **58**, 2059 (1987).
2. M. M. Sigalas and E. N. Economou, J. Sound Vibr. **158**, 377 (1992).
3. A. A. Karabutov, Jr., Yu. A. Kosevich, and O. A. Sapozhnikov, Acoust. Phys. **59**, 137 (2013).
4. Yu. I. Bobrovnitskii, Acoust. Phys. **57**, 442 (2011).
5. P. Yeh, *Optical Waves in Layered Media* (Wiley, New York, 1998).
6. Z. Liu, C. T. Chan, P. Sheng, A. L. Goertzen, and J. H. Page, Phys. Rev. B: Condens. Matter Mater. Phys. **62**, 2446 (2000).
7. F. K. Thomas, R. M. de la Rue, Progress in Quantum Electronics **23**, 51 (1999).
8. Z. Y. Liu, X. Zhang, Y. Mao, et al., Science **289**, 1734 (2000).
9. M. S. Kushwaha, P. Halevi, L. Dobrzynski, et al., Phys. Lett. **71**, 2022 (1993).
10. Y. T. Fang and T. G. Shen, Chin. Phys. Lett. **22**, 949 (2005).
11. X. D. Zhang, Phys. Rev. B: Condens. Matter Mater. Phys. **70**, 195110 (2004).
12. Y. T. Fang and Z. C. Liang, Opt. Commun. **283**, 2102 (2010).
13. H. Wang and Y. T. Fang, Eur. Phys. J. Appl. Phys. **52**, 30703 (2010).
14. Q. N. Liu, Science Sin.-Phys. Mech. Astron. **42**, 116 (2012).
15. Q. N. Liu, Mech. Sci. Technol. Aerospace Eng. **31,** 178 (2012) [in Chinese].
16. A. Yariv, Y. Xu, R. K. Lee, and A. Scherer, Opt. Lett. **24**, 711 (1999).
17. S. Feng, J. M. Elson, and P. L. Overfelt, Opt. Express. **13**, 4113 (2005).